Cold Regions Science and Technology 155 (2018) 58–68

Contents lists available at ScienceDirect

Cold Regions Science and Technology

journal homepage: www.elsevier.com/locate/coldregions

Changing runoff generation in the source area of the Yellow River: Mechanisms, seasonal patterns and trends

Xiaoling Wu[a,b,*], Xin Zhang[a], Xiaohua Xiang[a,b], Ke Zhang[c,d], Huijun Jin[e], Xi Chen[a,b], Chuanhai Wang[a,b], Quanqin Shao[f], Wenjuan Hua[a]

[a] College of Hydrology and Water Resource, Hohai University, Nanjing 210098, China
[b] State Key Laboratory of Hydrology-Water Resources and Hydraulic Engineering, Hohai University, Nanjing 210098, China
[c] Cooperative Institute for Mesosacle Meteorological Studies, University of Oklahoma, OK 73072, USA
[d] Hydrometeorology & Remote Sensing (HyDROS) Laboratory and School of Civil Engineering and Environmental Sciences, University of Oklahoma, Norman, OK 73072, USA
[e] State Key Laboratory of Frozen Soils Engineering, Cold and Arid Regions Environmental and Engineering Research Institute, Chinese Academy of Sciences, Lanzhou 730000, China
[f] Institute of Geographic Sciences and Natural Resources Research, CAS, Beijing 100101, China

ARTICLE INFO

Keywords:
Active layer
Freeze-thaw
Runoff generation
Climate change
Yellow river

ABSTRACT

The hydrological regimes of the major rivers in cold regions of the world have changed remarkably since the 1960s, but the mechanisms underlying these changes have not yet been fully understood. Specifically, changes in freeze-thaw processes can affect the thicknesses of the permafrost layer and active layer, storage capacity for liquid water and subsequent surface runoff. In this study, we investigated the hydrological processes and runoff generation in the Yellow River source (YRS) region, which is located in a permafrost region, over the past four decades using ground observations. The impacts of runoff processes are assessed in terms of the spatiotemporal distributions of precipitation, air temperatures, and soil water dynamics in the active layer. The Mann-Kendall test and correlation analysis were employed to detect the variations in runoff and annual changes in influencing factors. Runoff generation in different periods was influenced by different main factors. In the spring flood and recession flow period (SP_FRP, which ranges from late March to mid-June), soil water storage played an important role in runoff generation. With the increased air temperature and enhanced soil ground thawing process, liquid water storage capacity of the soil increased, and constrained runoff. After the soil was saturated in the summer flood and recession flow period (SU_FRP, which ranges from late June to late October), runoff increased with precipitation. In the dry period (DP, which ranges from early November to Mid-March), little precipitation, high potential evaporation (308 mm) and increased air temperature (0.43 °C/decade) caused decreases in snow accumulation and water content. Without a sufficient water supply, river runoff decreased in DP. These results show that precipitation played an important role in runoff generation in SU_FRP. In permafrost regions, the freeze-thaw processes of the active layer of soils, heavy evaporation and the air temperature play primary roles in runoff generation during SP_FRP and DP.

1. Introduction

Cold regions on the earth are believed to be the most sensitive to climate change. Global warming has led to remarkable changes in permafrost environments IPCC (International Panel on Climate Change), 2007; Jin et al., 2009; Harris et al., 2009). These changes include increases in soil temperature, deepening active layer thickness and thawing of permafrost (Harris et al., 2003; Jin et al., 2007a, 2007b; Marchenko et al., 2007). These changes have substantially altered the water cycles and ecosystems in these areas (McGuire, 2002; Walker et al., 2003; Jin et al., 2000; Jorgenson et al., 2001; Harris et al., 2001; Heginbottom, 2002; Romanovsky and Osterkamp, 2001; ARCPTF, 2003). Climate change-induced changes in active layers and permafrost are influencing seasonal runoff patterns and provide climate system feedbacks, and such feedbacks have received much attention from many international organizations and research projects (Zhao et al., 2010; Shiklomanov et al., 2008; Romanovsky and Osterkamp, 1997; Osterkamp and Romanovsky, 1997; Zhang et al., 2007; Wu and Zhang,

* Corresponding author at: College of Hydrology and Water Resource, Hohai University, Nanjing 210098, China.
E-mail address: freebir7237@sina.com (X. Wu).

https://doi.org/10.1016/j.coldregions.2018.06.014
Received 15 November 2016; Received in revised form 20 June 2018; Accepted 29 June 2018
Available online 07 July 2018
0165-232X/ © 2018 Elsevier B.V. All rights reserved.

2010; Romanovsky and Osterkamp, 1995; Shiklomanov et al., 2010; Li et al., 2012; Zhou et al., 2013; Yang et al., 2014).

During the past few decades, field measurements of climate conditions and hydrological processes in the cold regions have become more numerous (Dirksen, 1964; Hoekstra, 1966; Mao et al., 2003; Guo et al., 2002), but most of the measured data are either too short, sparse or discontinuous to capture changes in these factors. Mathematical models, such as the simple biosphere model (SiB) (Xue et al., 1991), biosphere-atmosphere transfer scheme (BATS) (Dickinson et al., 1993), simultaneous heat and water model (SHAW) (Flerchinger and Saxton, 1989a, 1989b; Flerchinger et al., 1998), variable infiltration capacity model (VIC) (Liang et al., 1994) and cold regions hydrological model (CRHM) (Pomeroy et al., 2007; Zhou et al., 2014), have used been to model critical hydrological processes, such as snow accumulation, snow melting, and water and heat transfer in freezing-thawing soil layers, in cold regions. The freezing-thawing processes of the active layers and their interactions with air temperature and precipitation are particularly important but relatively poorly implemented in current models. For example, most macro-scale hydrological models and land surface models do not account for soil thermal-moisture dynamics or runoff (Zhuang et al., 2004; Nicolsky et al., 2007; Yi et al., 2009).

Because the presence of permafrost prevents liquid water from percolating down to deep soils, permafrost regions are commonly characterized by higher water yield ratios and larger direct runoff ratios for the same levels of rainfall and snowmelt than unfrozen and temperate regions (Hayashi et al., 2003). The flow discharges of Eurasian arctic rivers have increased during the past 70 years (Peterson et al., 2002) and are projected to continuously increase in the future as the air temperature rises (Peterson et al., 2002). Singh and Singh (2001) believed that a catchment's hydrology is strongly governed by snow thickness in the snow-covered area. Stream water quality and runoff depend on snow accumulation and ablation processes (Tranter and Jones, 2001; Woli et al., 2008), but it is unclear how the thawing of permafrost affects runoff processes (Zhang and Barry, 2003; McClelland et al., 2004). McNamara et al. (1998) and Carey and Woo (2001) found that the surface water yield ratio increased two-fold if the thickness of the active layer is deepen from 0.6–2.0 m to 0.4–0.6 m.

The objectives of this study are (1) to identify relationships between the hydrological processes and environmental factors in the source area of the Yellow River, (2) to reveal the responses of the runoff generation process to different atmospheric conditions, and (3) to determine the effects of freeze-thaw processes on runoff generation in this region.

2. Data and methodology

2.1. Site description

Our study region is the source area of the Yellow River (SAYR), which is located on the Qinghai-Tibet Plateau and ranges from 32°43′N to 35°44′N and 95°46′E to 102°38′E with a contributing area of $1.219 \times 10^5\,km^2$. The highest and lowest points in the SAYR catchment are 6300 m and 1400 m above mean sea level, respectively (Chen et al., 2006; Lan et al., 2010; Guo et al., 2013). With a high average elevation and complex topography (Fig. 1), the SAYR has a distinctive atmospheric circulation pattern that profoundly affects both the regional and global climate (Cheng, 1984; Zhao and Qian, 2007; Wang et al., 2008). The SAYR has continental climate characteristics, such as strong radiation, long sunshine hours, alternating warm and cold seasons, and periodic wet and dry conditions. In the summer, it is rainy and wet in the SAYR under the influence of the southwest monsoon. In the winter, this region is dry and cold under the influence of the Qinghai-Tibet cold high-pressure system. The SAYR, a major water source, is the largest area supplying water to the Yellow River watershed in terms of snowmelt and precipitation (Qian et al., 2004).

As shown in Fig. 1, two hydrological stations, JiMai and Tangnag, are located at the center and outlet of the SAYR, respectively. The SAYR is divided into upstream and downstream reaches by JiMai. The contributing areas for the two sites are $4.415 \times 10^4\,km^2$ and $1.219 \times 10^5\,km^2$, respectively (Shao and Fan, 2012). The measured meteorological variables at these sites include hourly precipitation, air temperature, evaporation, relative humidity, wind speed, sunshine hours and atmospheric pressure.

The primary soil types are sandy loam, clay loam and silty clay loam. Sandy loam and clay loam appear in both surface and deep soil layers, while silty clay loam is always found in deep layers (Shao et al., 2009). The soil in this region is seasonally frozen with spatially varied permafrost. Large amounts of permafrost are buried in the upstream area of the SAYR. At Darlag, the daily snow thickness and soil freezing depth were observed. Soil temperatures at the surface (5 mm below the surface) and at depths of 5, 10, 15 and 20 cm below the ground surface were monitored from January 2005 to December 2007. The unfrozen water content in soil at depths of 10, 20, 30, 40 and 50 cm was measured by time-domain reflectometry (TDR) every 8 days. The TDR gives the volumetric liquid water content in thawed soils and the volumetric unfrozen water content in frozen soils. Weighing lysimeters are usually used to determine the land surface evaporation (ET) (Zhang et al., 2003a, 2003b).

2.2. Methods

The Mann-Kendall (MK) test (Mann, 1945; Kendall, 1975) was applied to detect trends in the recorded hydrologic time series data on precipitation, air temperature, evaporation and runoff time series. The MK test statistic (S) is defined as:

$$S = \sum_{i=1}^{n-1} \sum_{j=i+1}^{n} sgn(x_j - x_i) \tag{1}$$

$$sgn(x_j - x_i) = \begin{cases} 1 & x_j > x_i \\ 0 & x_j = x_i \\ -1 & x_j < x_i \end{cases} \tag{2}$$

where x_i and x_j are the data values at times i and j and n indicates the length of the dataset. When n is > 10, the standard Z value is calculated according to the following equation:

$$Z = \begin{cases} \frac{S-1}{\sqrt{Var(S)}} & S > 0 \\ 0 & S = 0 \\ \frac{S+1}{\sqrt{Var(S)}} & S < 0 \end{cases} \tag{3}$$

The calculated standard Z value is compared with the standard normal distribution table with two-tailed confidence levels ($\alpha = 10\%$, $\alpha = 5\%$, $\alpha = 1\%$). If the calculated Z is greater than $|Z| > |Z_{1-\alpha/2}|$, the null hypothesis is invalid. When the absolute value of Z is greater than or equal to 1.28, 1.64 and 2.32, the significance test passes with a confidence level of 90%, 95% and 99%, respectively.

The concentration index (CI)

To determine the relative impact of different classes of daily precipitation and to evaluate the weight of the largest daily event in the total precipitation value, it is necessary to analyze the accumulated percentages of precipitation (Y) contributed by the accumulated percentages of days (X) during Y's occurrence (Riehl, 1949; Olascoaga, 1950; Martin-Vide, 2004; Zhang et al., 2009; Li et al., 2010). If daily events are ranked in decreasing order and Xj is the jth highest event, Yj is the fraction of annual precipitation provided by the greatest events from the 1st to the jth. If X events are expressed in terms of percentiles and Y is expressed in terms of percentage of annual precipitation, Y and X are linked by an exponential law, as (Riehl, 1949; Olascoaga, 1950):

$$Y = aX\ exp\ (bX) \tag{4}$$

where a and b are constants. Generally, this curve is called the concentration curve or Lorenz curve (Shaw and Wheeler, 1994) and is also

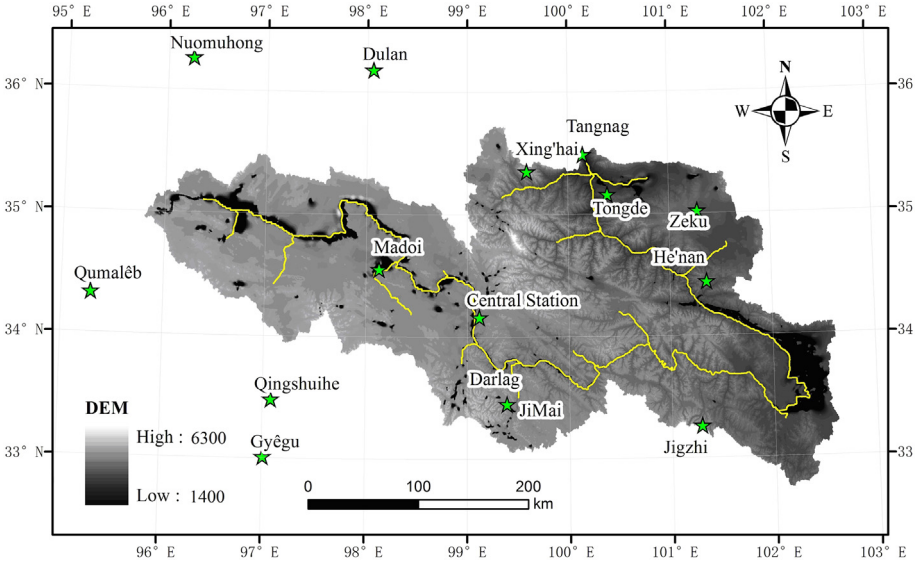

Fig. 1. The topographic map of the SAYR and the locations of observation sites.

known as the normalized rainfall curve (Jolliffe and Hope, 1996) when referring to precipitation. The Lorenz curve can be evaluated as follows:

$$CI = \left\{5000 - \left[\frac{a}{b}e^{bx}\left(x - \frac{1}{b}\right)\right]_0^{100}\right\}/5000 \quad (5)$$

The procedure used in this work analyzes the daily data distribution for each rain station using a limit of 1 mm/day as the precipitation class interval. A high precipitation CI value indicates that precipitation is more concentrated within a few rainy days during the year and vice versa.

To investigate the spatial distribution of precipitation, evaporation and air temperature in the SAYR, inverse distance weighted (IDW) interpolation was used to predict a value for any unmeasured location in the SAYR. The interpolated data include trends in seasonal precipitation, trends in seasonal air temperatures, the total amount of precipitation and the mean annual air temperature (MAAT).

To identify the primary factors influencing surface runoff processes during different periods, a correlation analysis was conducted to assess the relations between runoff and environmental variables. During the snow melting period, the observed snow cover and air temperature were also taken into account to identify the primary factors contributing to flood runoff, especially for the SP_FRP runoff.

3. Results and discussion

3.1. Characteristics of runoff changes during 1960–2007

The mean annual runoff volume of this region is approximately $2.02 \times 10^{10}\,m^3$, accounting for ~38.5% of the runoff of the Yellow River basin (Shao and Fan, 2012). The annual total runoff of the SAYR decreased significantly by $5.5 \times 10^9\,m^3$ from 1960 to 2007. The changes in runoff in the SAYR exhibit large seasonal differences. Over these 48 years, the runoff in SU_FRP (from June 11th to October 31st) decreased by $3.8 \times 10^9\,m^3$, which accounts for approximately 70% of the total amount of decrease in annual total runoff. The decrease in the SU_FRP runoff is much higher than the runoff decreases in DP (from November 1st to March 20th) and SP_FRP (from March 21st to June 10th), which account for 17% and 13% of the total decrease in annual runoff over the study period, respectively. Over the same period, the mean annual rainfall in the SAYR approached 500 mm, and the regional annual rainfall increased by 0.07 mm/decade with large spatial variabilities. However, the precipitation increased in SP_FRP and DP during the study period at an average rate of 0.13–9.35 mm/decade (Fig. 2), and annual evaporation decreased by 15.3 mm/decade. Based on multi-year precipitation information, most of the SAYR exhibited an increasing precipitation trend in SP_FRP and DP except for the eastern SAYR near Henan, where multi-year precipitation decreased in SP_FRP at a rate of −0.223 mm/year (Fig. 2). In contrast with the trend in the SP_FRP and DP, most of the SAYR exhibited a decreasing trend in precipitation in SU_FRP. In SU_FRP, the southern part of the basin (around Jigzhi) exhibited a considerable decrease in precipitation, and the average precipitation in Jigzhi in the 1990s was 475.2 mm lower than that in the 1980s (576.1 mm). This difference may have been due to the effects of climate warming on precipitation in the southern part of the basin (Fig. 2).

To study the seasonal changes in precipitation, the spatiotemporal patterns of the concentration index (CI) were analyzed. A high precipitation CI means that a large percentage of the yearly total precipitation occurred within a few days (Coscarelli and Caloiero, 2012).

First, the precipitation CI values were estimated for each year for all the stations, and then, the average values for each station were obtained. The mean annual values of CI range from a minimum of 0.52 to a maximum of 0.61.

In the DP, the CI distribution is not uniform: high CI values were observed in the south, with a peak value (0.59) at Darlag station (Fig. 3c). Compared with that in DP, the spatial distribution of CI in SU_FRP is similar to that in SP_FRP. In SP_FRP, the highest CI values (0.61) were in the northern and western SAYR, but the southeastern region exhibited the lowest value of CI (0.57) (Fig. 3a). The topography influences the distribution of precipitation, which may explain the differences in SP_FRP and SU_FRP CI values, which decline from northwest to southeast.

Despite the similar patterns between SU_FRP and SP_FRP, the spatial distribution of seasonal precipitation regimes also changed. For rainfall in SU_FRP, most parts of the region exhibited high CI values ranging from 0.55 to 0.6 (Fig. 3b).

The correlation between runoff and precipitation in SU_FRP was high ($r = 0.78$) (Fig. 4b, h), suggesting that the runoff in SU_FRP mainly relies on local rainfall. The largest runoff values and heaviest annual precipitation occurred in the same years. Along with the decreasing trend (−0.73 mm/year) of SU_FRP precipitation, the SU_FRP runoff ($-8.76\,m^3/s$/year) at Tangnag (the outlet of the SAYR) exhibited a large decreasing trend, suggesting that change in SU_FRP precipitation is the main cause of the decreasing SU_FRP runoff in this region (Fig. 4).

Although precipitation and runoff in SU_FRP exhibit the same

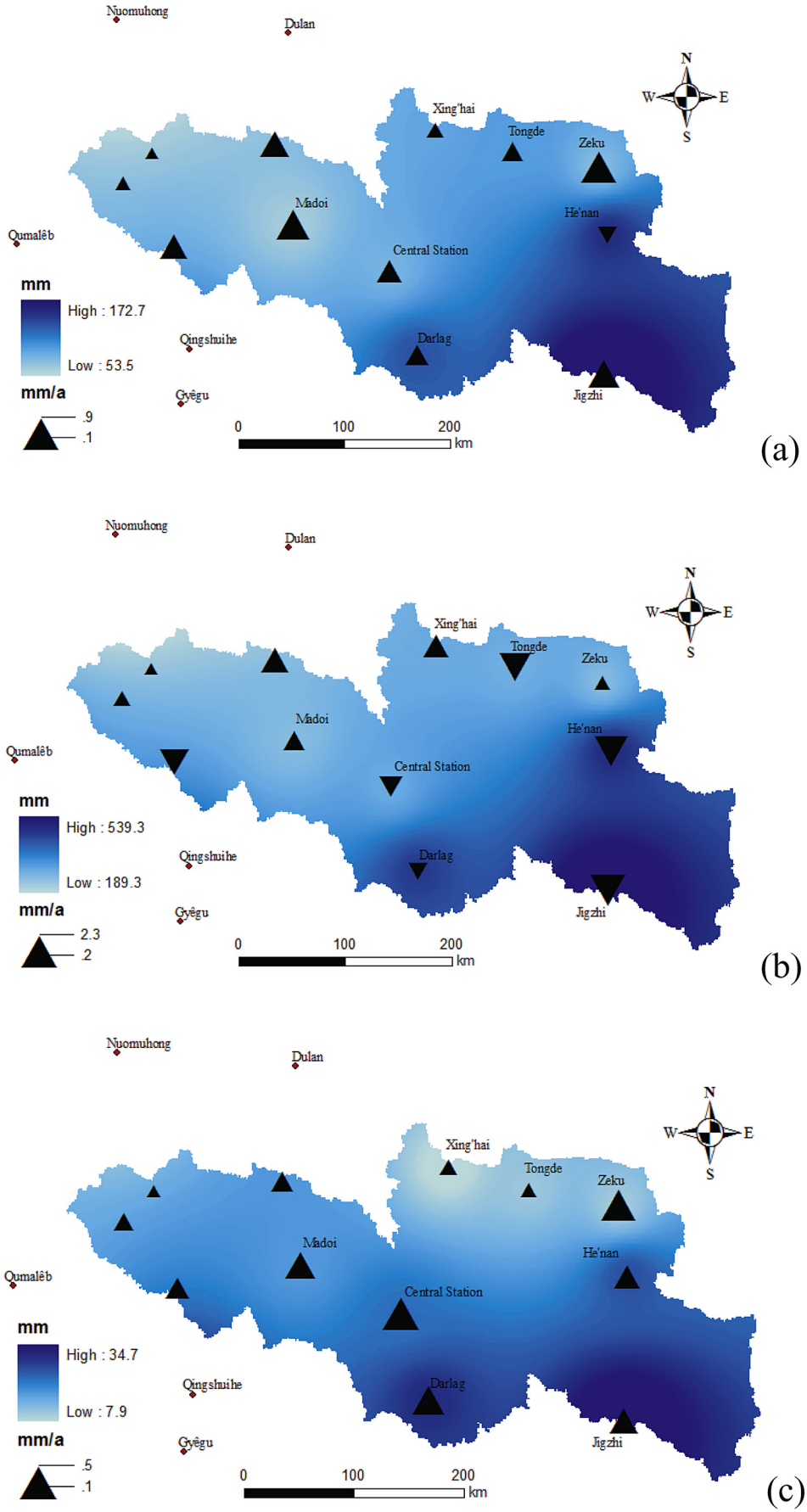

Fig. 2. Spatial distribution of multi-year mean annual precipitation in the SAYR in the three periods: (a) SP_FRP, (b) SU_FRP, and (c) DP. The triangle represents the trend; an upward-pointing triangle represents an increase and vice versa.

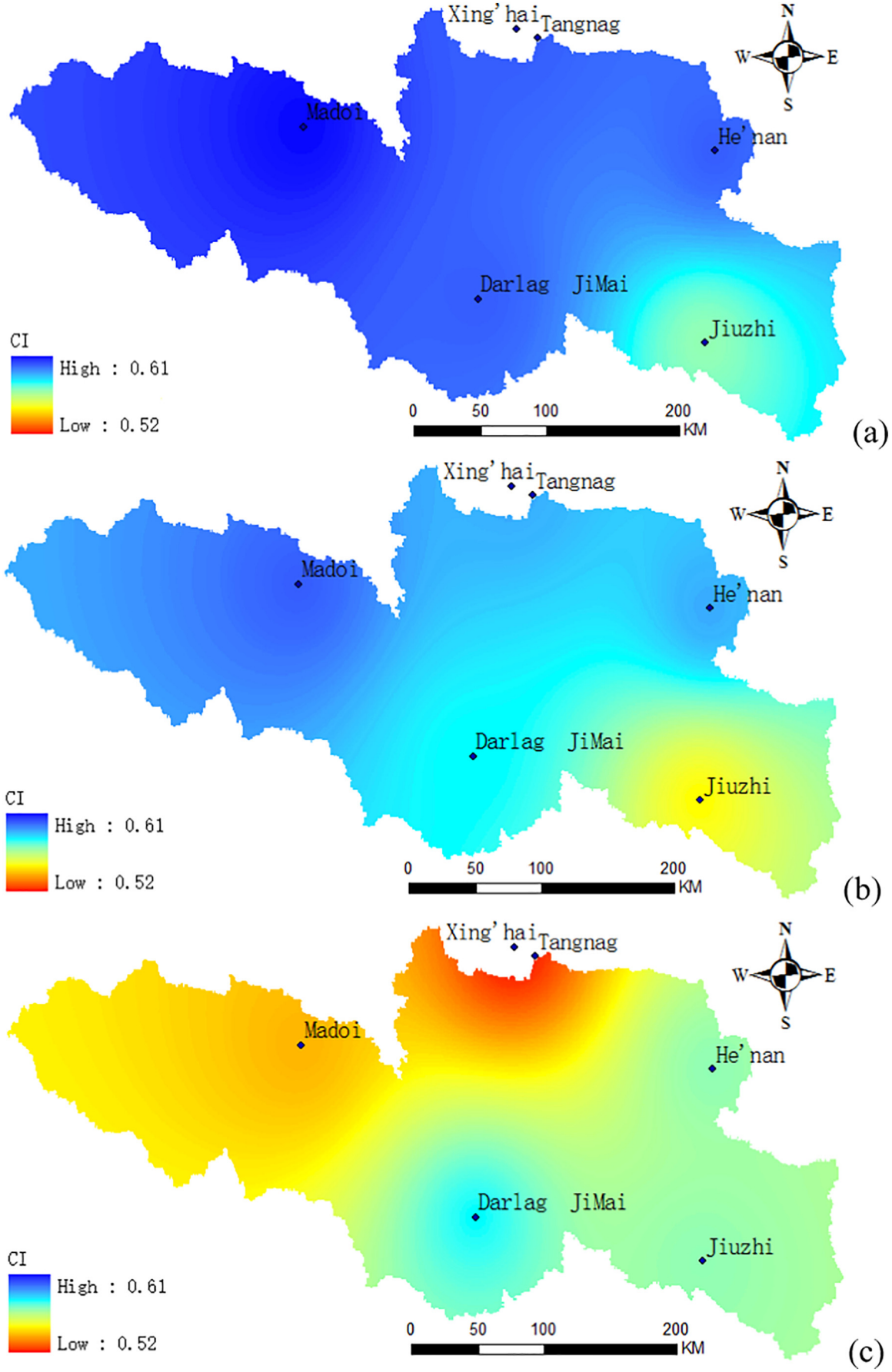

Fig. 3. Spatial distribution of the multi-year mean annual CI in the SAYR for the three periods: (a) SP_FRP, (b) SU_FRP, and (c) DP.

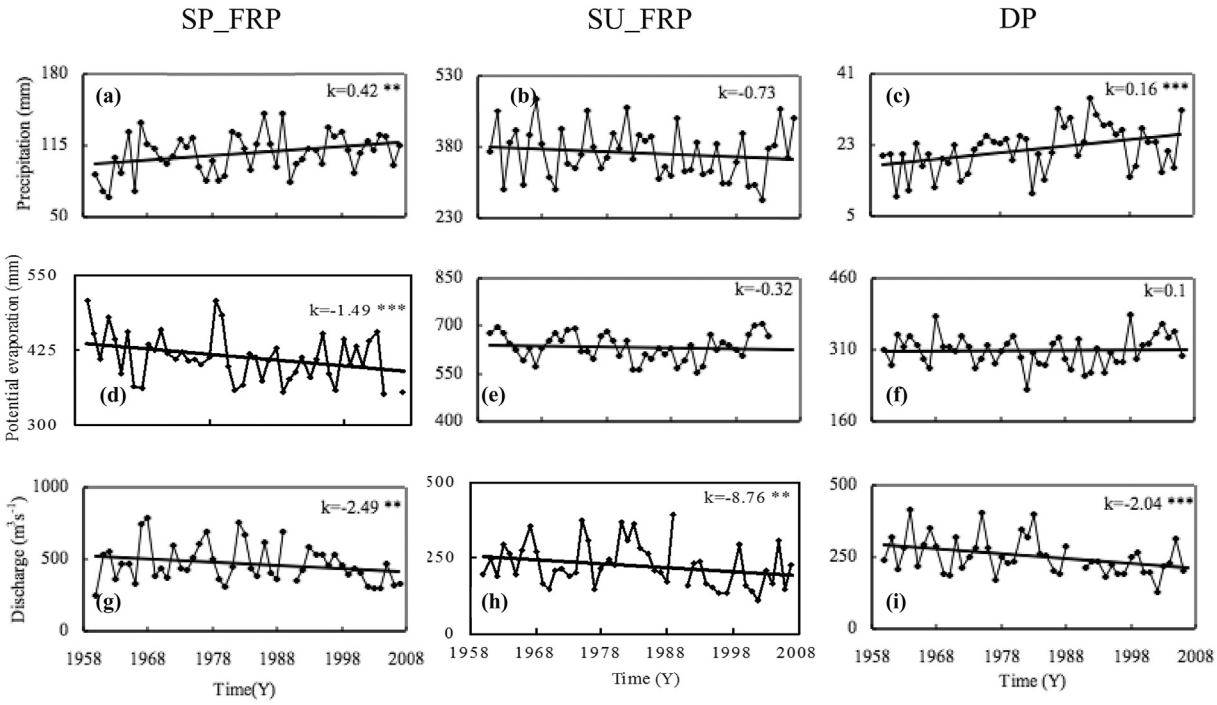

Fig. 4. Time series and temporal trends of (a, b, c) annual total precipitation; (d, e, f) potential evaporation of the SAYR watershed in SP_FRP, SU_FRP, and DP from 1960 to 2007; and (g, h, i) annual total runoff measured at Tangnag (outlet of the SAYR watershed) in the three periods. $*P < .1$; $**p < .05$; $***p < .01$.

change trend, these factors exhibit opposite trends in both SP_FRP and DP: precipitation shows significant upward trends in the two periods over the 48 years (Fig. 4a, c), while runoff exhibits significant downward trends over the same period (Fig. 4 g, i). Interestingly, evaporation in the SP_FRP also exhibits a negative trend. However, most of the SAYR experiences increasing precipitation in SP_FRP, especially in the upstream and downstream reaches, with the highest upward trend reaching 0.9 mm/year. Water influx in the SP_FRP increased over the 48 years and water effluxes (ET and runoff) decreasing over the same period. We also computed the runoff coefficient (the ratio of runoff to precipitation) over this period to infer seasonal differences in runoff generation. The average runoff coefficient in SP_FRP (0.26) is smaller than that in SU_FRP (0.3) because surplus water is accumulatively stored on and/or under the ground, which perhaps indicates that a portion of precipitation in SP_FRP is snow due to the cold temperatures and thus can be stored on the ground surface while another portion is stored in the thawing soil. At the same time, the precipitation in SU_FRP is almost all in liquid form and can directly contribute to runoff. In other words, changes in soil water storage are likely to play an important role in regulating runoff generation in SP_FRP in this area.

The runoff coefficient in DP (1.29) is larger than 1 because precipitation in this period is low and runoff is mainly from the water storage on the surface and under the ground. The runoff coefficients of all the three periods show negative trends over the 48 years (Fig. 5), suggesting that a greater proportion of precipitation in this region is allocated to water storage given that the ET in this region does not exhibit an upward trend (Fig. 4).

3.2. Warming in the SAYR

The SAYR is a cold region with an average of 200 days below an air temperature of 0 °C. Changes in water storage in this region are mainly controlled by the thickness of active layers. Seasonal freezing and thawing processes are greatly influenced by air temperature. Therefore, we analyzed changes in air temperature across this region. MAAT increased by 0.38 °C/decade, with warming during SU_FRP of 0.34 °C/decade and warming during SP_FRP of 0.24 °C/decade. The multi-year trend in MAAT at all air temperature stations varied from 0.16 °C/decade to 0.4 °C/decade, and according to the MK test, these trends were significant at the significance level of 99% (Fig. 6). A significant warming occurred in DP. The average rate of air temperature increase in DP was approximately 0.43 °C/decade.

Due to the decreased precipitation and high potential evaporation (the multi-year mean potential evaporation in SU_FRP is 634.2 mm), the runoff decreased in SU_FRP. Because the air temperature dropped below zero, the soil began to freeze, and runoff entered a recession flow period with a higher runoff coefficient. In DP, accompanied by yearly increasing air temperature, strong potential evaporation and little precipitation, the multi-year mean annual runoff from 1960 to 2007 decreased dramatically (from 3.6×10^9 m^3 to 2.6×10^9 m^3), especially after the 1980s.

To determine the main factors influencing runoff generation, especially during the period of soil thawing (SP_FRP) and freezing (DP), the upstream reaches of the SAYR were taken as the study object. Permafrost was present in much of the upstream basin (Zhao et al., 2017). The analysis focused on the thawing and freezing process in the active layer (including freezing/thawing starting time, water content and freezing/thawing depth).

3.3. The influences of thawing on SP_FRP runoff

To identify the impacts of the freeze-thaw cycles on runoff generation, we investigated the observed air temperature, evaporation, snow cover, soil water content, freezing depth at Darlag, regional precipitation (interpolated by the tessellation method with polygons to get the regional average precipitation) and discharge at JiMai station, which is located in the upstream reaches of the SAYR (Fig. 1). In Fig. 7, it can be seen that runoff varies considerably, especially from March to June 2006. Because the active layer thaw depth deepened from 0 to 1.72 m during the thawing period, the runoff at JiMai decreased from 101 m^3/s to 46.6 m^3/s.

At Darlag, because the soil began to thaw in late March 2006, a portion of the meltwater and precipitation was stored in soil, and another portion became runoff in SP_FRP.

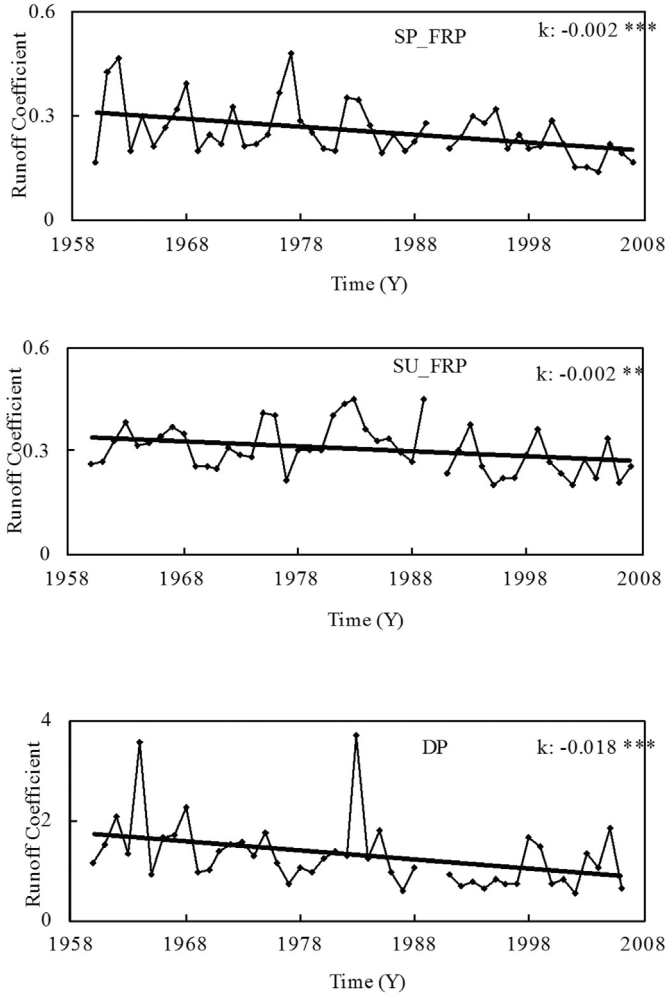

Fig. 5. Yearly runoff coefficients for the three periods in SAYR from 1960 to 2007, *P < .1; **p < .05; *** < p < .01.

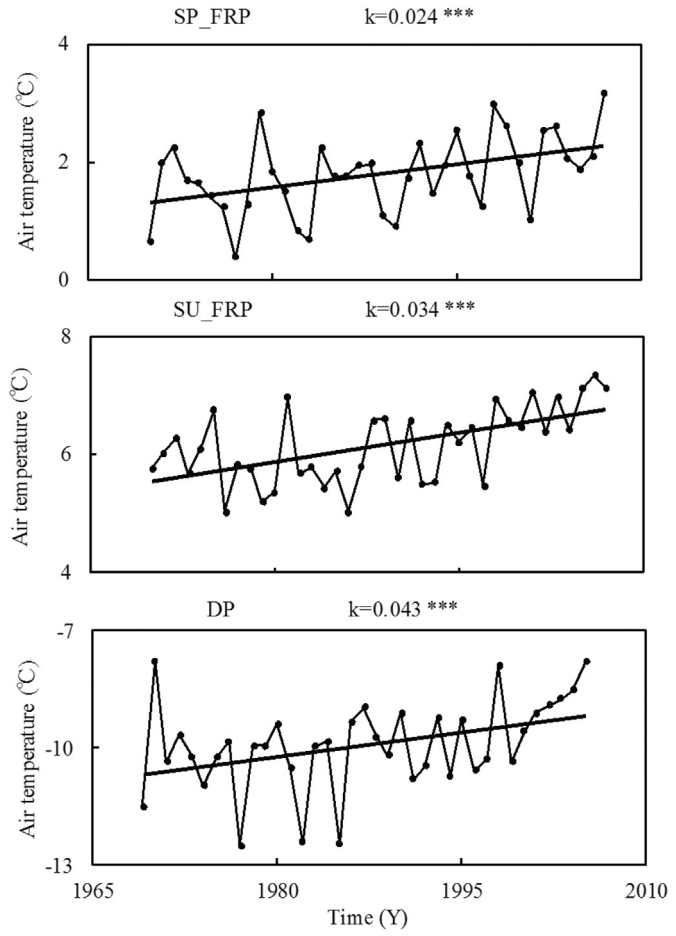

Fig. 6. Yearly air temperature for the three periods in SAYR from 1970 to 2007, *P < .1; **p < .05; *** < p < .01.

In early April, snowpack gradually began to melt as the air temperature increased (Fig. 7). The observed discharge at JiMai began to increase and peaked in early May. Because the active layer thawed completely in May, the ratio of runoff to precipitation in May (0.24) was lower than that in April (0.43) and March (0.53), indicating that a larger proportion of precipitation was stored during late SP_FRP. Along with the increased air temperature, ET also increased from 2.8 mm (early May) to 7.4 mm (late May). The active layer did not thaw completely until late May. Influenced by the strong evaporation, the soil moisture of the top layer decreased gradually. Supplied by precipitation infiltration in mid and late May, the liquid water content raised gradually, especially in the shallow soil layer (0–0.1 m), with the soil water content change from 17.1% (late May) to 28.2% (early June). In June, the soil water content exceeded the field water capacity (23%) (Yi et al., 2012). The ratio of runoff to precipitation in June reached the lowest value (0.21) of the year.

The thawing process, which causes the soil layers to become porous, permeable, is accompanied by snowmelt and thus enhances infiltration. As a result, although precipitation and snowpack melt in the warm season (in late May), runoff at JiMai does not increase substantially (55 m^3/s, which is only half of the peak value in early May) until early June, when the soil becomes saturated. The thawing process is mainly controlled by air temperature. As the air temperature increases, the thawing process speeds up, and the maximum thaw depth deepens, resulting in increased soil water-holding capacity and increased liquid water storage capacity at the watershed level. Portions of precipitation and snowmelt were stored in enlarged, thawed soil layers as temperature increased, which lead to a decreased runoff coefficient. After the soil became saturated (water content reaches the field water capacity), direct runoff generation occurred. These results suggest that in addition to precipitation and evaporation, the air temperature has a great effect on runoff in SP_FRP, especially in period when the active layer is thawing.

3.4. Influences of soil freezing on DP runoff

For the runoff process in this cold region, DP is the recession period. Because this period is characterized by little precipitation, cold temperatures, strong evaporation and freezing processes, the runoff at JiMai decreased gradually from 94.5 to 15.4 m^3/year from November to mid-December 2006. During this cold period, when evaporation temporarily rises (from the 1st to 6th of December), without any human activity, the runoff at JiMai decreased from 44.8 to 15.4 m^3/s, which indicates that in this short period of variation in runoff, the high levels of evaporation will constrain the water output capacity of the basin (Fig. 8).

3.4.1. Several factors may impact the decrease in runoff in DP

First, the air temperature increased 0.43 °C/decade during DP in the SAYR from 1960s to 2000s. Chen et al. (2007) found that the degeneration of permafrost caused the water level of frozen crusts to descend. Permafrost can prevent precipitation from infiltrating to deeper soils and can keep the groundwater table high. As the active layer thickness deepens with increasing air temperature, the groundwater table continues to lower. The evaporation or infiltration of shallow soil moisture

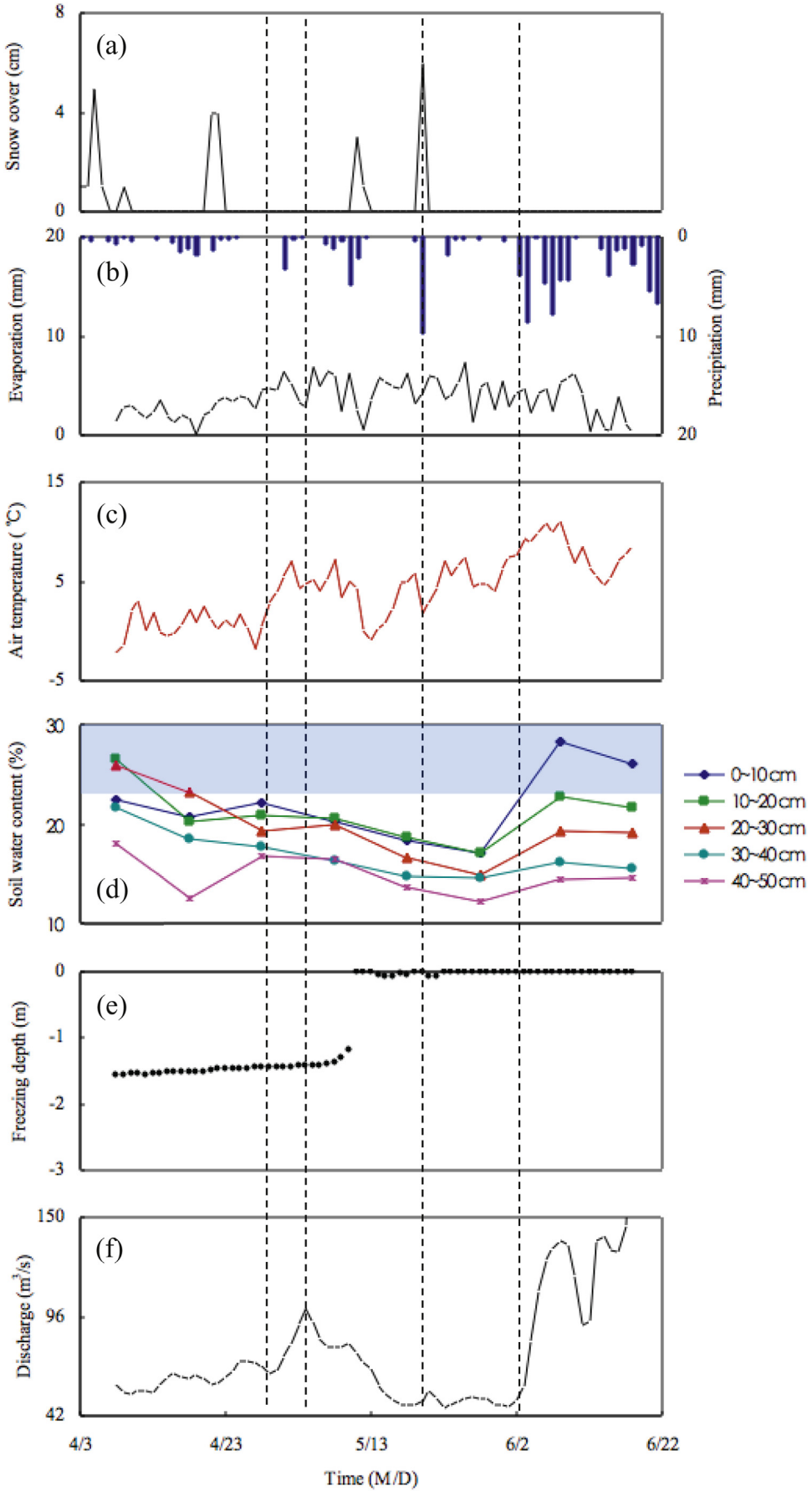

(caption on next page)

Fig. 7. Time curves of observed (a) daily snowpack depth at Darlag, (b) daily ET at Darlag (black solid line) and precipitation in the upstream basin of SAYR (blue bars), (c) daily mean air temperature at Darlag, (d) daily soil water content at five depths and the field water capacity at Darlag (blue bar), (e) daily freezing depth at Darlag, and (f) daily flow discharge of the upstream basin of SAYR collected at JiMai from April 3 to June 22 in 2006. (For interpretation of the references to colour in this figure legend, the reader is referred to the web version of this article.)

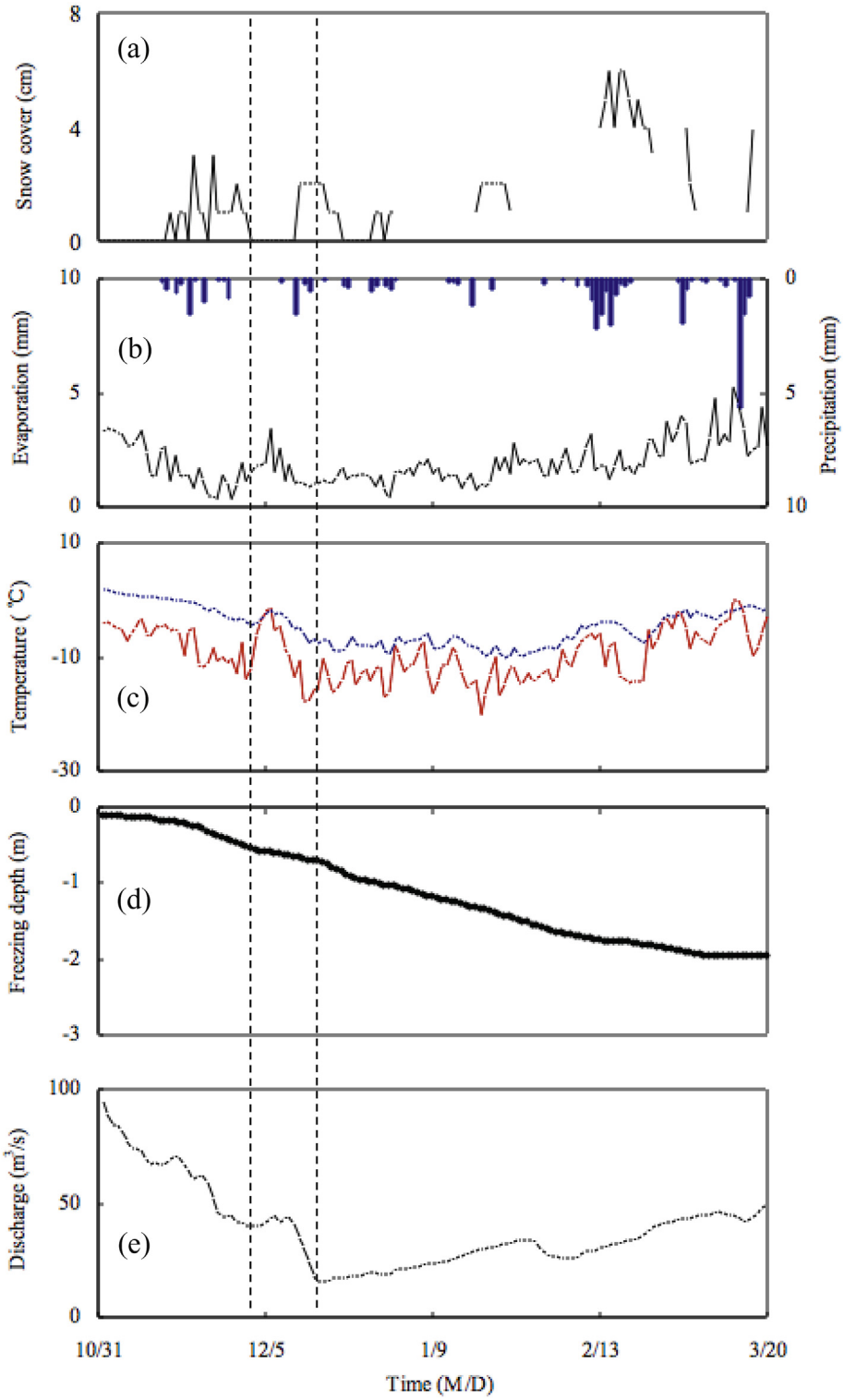

Fig. 8. Time curves of observed (a) daily snowpack depth at Darlag, (b) daily ET at Darlag (black solid line) and precipitation in the upstream basin of SAYR (blue bars), (c) daily mean air temperature at Darlag (red solid line) and soil temperature at depth of 20 cm at Darlag (blue solid line), (d) daily freezing depth at Darlag, and (e) daily flow discharge of the upstream basin of SAYR collected at JiMai from October 31, 2006 to March 20 in 2007. (For interpretation of the references to colour in this figure legend, the reader is referred to the web version of this article.)

into lower soil layers will decrease in arid conditions because the groundwater table moves downwards.

Second, the heavy evaporation continued to increase in the SAYR after the 1980s, and the potential evaporation significantly increased (2.17 mm/year). According to the MK test, this trend was found to be significant at the significance level of 95%. Compared with precipitation, the evaporation was high in DP. The mean annual ratio of potential evaporation to precipitation reached 15.4.

Third, in the form of snow or ice, precipitation in DP cannot directly generate in the same period. Given the high runoff coefficient in DP (Fig. 5), the runoff was mainly from the base flow in SU_FRP. The runoff decreased in SU_FRP (Fig. 4 h), and with a limited water supply, the runoff in DP decreased.

Finally, the increased air temperature, potential evaporation and decreased runoff in SU_FRP together contributed to decreasing the runoff in DP.

Some observations indicated that there was a rapid transition of permafrost from stable to unstable and from continuous to discontinuous as the temperatures increased from the 1980s to 2000s (Zhao et al., 2017). The boundary between permafrost and seasonal frozen soil is moving both northward and westward. With the thawing and freezing of soils, runoff varies greatly. Therefore, variations in the thawing-freezing processes of the active layer soils and the permafrost degradation play an important role in seasonal shifts of runoff in the SAYR.

4. Conclusions

Surface runoff processes in the SAYR exhibited different characters. The temporal and spatial distributions of precipitation, evaporation, air temperature and soil freezing-thawing status were taken into consideration for runoff generation.

During the thawing process, the liquid water storage capacity increases along with the soil water phase change. Dominated by the increase in temperature, the thawing of the active layer was sped up, and the maximum thaw depth deepened, which in turn increased the soil water-holding capacity and enhanced the water storage capacity of the watershed. As a result, even with precipitation and snowmelt in the warm season, runoff at JiMai does not vary significantly until SU_FRP, when the thawing process is complete.

The second reason for the decrease in runoff was the strong evaporation, which dropped soil surface moisture quickly. Driven by the annually increasing air temperature, the melting active layer was another reason for the decrease in runoff in DP. With the degradation and disappearance of permafrost, the groundwater table has moved downward. The soil moisture decreased because of the lowering of the groundwater table and strong evaporation. Therefore, variations in the thawing-freezing processes of the active layer soils play a significant role in the seasonal shifts of runoff in the SAYR.

Acknowledgments

This research is supported by the National Key R&D Programme of China (No. 2016YFA0601000), the Fundamental Research Funds for the Central Universities (No. 2018B10914) and the National Natural Scientific Foundation of China (No. 41571130071). Many thanks for the good advice and explanations on permafrost and the active layer from Professor French (Hugh French).

References

Carey, S.K., Woo, M.K., 2001. Slope runoff processes and flow generation in a subarctic, subalpine catchment. J. Hydrol. 253, 110–129.

Chen, L.Q., Liu, C.M., Yuan, F., 2006. Feasibility Study on Hydrologic Simulation in Basins with Macro2Scale Data Scarce. Resources science. Vol. 28 (1). pp. 87–92 in Chinese.

Chen, L.Q., Liu, C.M., Li, Y.P., Wang, G.Q., 2007. Impacts of climatic factors on runoff coefficients in source regions of the Huanghe River. Chin. Geogr. Sci. 17 (1), 47–55. https://doi.org/10.1007/s11769-007-0047-4.

Cheng, G.D., 1984. Problems on zonation of high-altitude permafrost. Acta Geograph. Sin. 39, 185–193 (In Chinese).

Coscarelli, R., Caloiero, T., 2012. Analysis of daily and monthly rainfall concentration in southern Italy (Calabria region). J. Hydrol. 416-417, 145–156.

Dickinson, R.E., Henderson-Sellers, A., Kennedy, P.J., 1993. Biosphere-Atmosphere transfer scheme (BATS) version le as coupled to the NCAR community climate model. In: National Center for Atmospheric Research Technical Note NCAR/TN-387 + STR. National Center for Atmospheric Research, Boulder.

Dirksen, D., 1964. Water movement and frost heaving in unsaturated soil without an external source of water. In: Department of Agronomy Cornell University, (Ph.D. thesis).

Flerchinger, G.N., Saxton, K.E., 1989a. Simulataneous heat and water model of a freezing snow-residue-soil system I. Theory and development. Transactions of the ASAE 32 (2), 565–571.

Flerchinger, G.N., Saxton, K.E., 1989b. Simulataneous heat and water model of a freezing snow-residue-soil system II. Field verification. Transactions of the ASAE 32 (2), 573–578.

Flerchinger, G.N., Kustas, W.P., Weltz, M.A., 1998. Simulating surface energy and radiometric surface temperatures for two arid vegetation communities using the SHAW model. J. Appl. Meteorol. 37 (5), 449–460.

Guo, Z.R., Jing, E.C., Nie, Z.L., Jiao, P.C., Dong, H., 2002. Analysis on the characteristics of soil moisture transfer during freezing and thawing period. Adv. Water Sci. 13 (3), 298–302.

Guo, L., Zhang, Y.X., Gao, Y.H., Hao, Z.C., Cairang, L.S., 2013. The impacts of climate change and land cover/use transition on the hydrology in the upper Yellow River Basin, China. J. Hydrol. 502, 37–52.

Harris, C., Haeberli, W., Mühll, V.D., King, L., 2001. Permafrost monitoring in the high mountains of Europe: the PACE project in its global context. Permafr. Periglac. Process. 12 (1), 3–11.

Harris, C., Mühll, V.D., Isaken, K., Haeberli, W., Sollid, J.L., King, L., Holmlund, P., Dramis, F., Guglielmin, M., Palacios, D., 2003. Warming permafrost in European mountains. Glob. Planet. Chang. 39 (3/4), 215–225.

Harris, C., Arenson, L.U., Christiansen, H.H., Etzemuller, B., Frauenfelder, R., Gruber, S., Haeberli, W., Hauck, C., Holzle, M., Humlum, O., 2009. Permafrost and climate in Europe: monitoring and modelling thermal, geomorphological and geotechnical responses. Earth Sci. Rev. 92, 117–171.

Hayashi, M., van der Kamp, G., Schmidt, R., 2003. Focused infiltration of snowmelt water in partially frozen soil under small depressions. J. Hydrol. 270, 214–229.

Heginbottom, J.A., 2002. Permafrost mapping: a review. Prog. Phys. Geogr. 26 (4), 623–642.

Hoekstra, P., 1966. Moisture movement in soil under temperature gradiens with the cold-side temperature under freezing. Water Resour. Res. 2, 241–250.

IPCC (International Panel on Climate Change), 2007. Climate change 2007: the physical science basis. Summary for policy makers. Fourth Assessment Report. Cambridge University Press, Cambridge, UK.

Jin, H.J., Cheng, G.D., Li, S.X., Zhao, L., 2000. Permafrost and climatic change in China. Glob. Planet. Chang. 26 (4), 387–404.

Jin, H.J., Yu, Q.H., Lü, L.Z., Guo, D.X., Li, Y.W., 2007a. Degradation of permafrost in the Xing'anling Mountains, Northeastern China. Permafr. Periglac. Process. 18 (3), 245–258.

Jin, H.J., Yu, Q.H., Wang, S.L., Lü, L.Z., 2007b. Changes in permafrost environments along the Qinghai–Tibet engineering corridor induced by anthropogenic activities and climate warming. Cold Reg. Sci. Technol. 53 (3), 317–333.

Jin, H.J., He, R.X., Cheng, G.D., Wu, Q.B., Wang, S.L., Lü, L.Z., Chang, X.L., 2009. Changes in frozen ground in the source area of the Yellow River on the Qinghai-Tibet plateau, China, and their eco-environmental impacts. Environ. Res. Lett. 4, 045206. https://doi.org/10.1088/1748-9326/4/4/045206.

Jolliffe, I.T., Hope, P.B., 1996. Representation of daily rainfall distributions using normalized rainfall curves. Int. J. Climatol. 16, 1157–1163.

Jorgenson, M.T., Racine, C.H., Walters, J.C., Osterkamp, T.E., 2001. Permafrost degradation and ecological changes associated with a warming climate in Central Alaska. Clim. Chang. 48 (4), 551–579.

Kendall, M.G., 1975. Rank Correlation Methods, 4th ed. Charles Griffin, (London).

Lan, Y.C., Zhao, G.H., Zhang, Y.N., Wen, J., Liu, J.Q., Hu, X.L., 2010. Response of runoff in the source region of the Yellow River to climate warming. Quat. Int. 226, 60–65.

Li, X., Jiang, F., Li, L., Wang, G., 2010. Spatial and temporal variability of precipitation concentration index, concentration degree and concentration period in Xinjiang, China. Int. J. Climatol. published online. https://doi.org/10.1002/joc.2181.

Li, R., Zhao, L., Ding, Y.J., et al., 2012. Temporal and spatial varia- tions of the active layer along the Qinghai–Tibet highway in a permafrost region. Chin. Sci. Bull. 57, 2864–2871.

Liang, X., Lettenmaier, D.P., Wood, E.F., 1994. A simple hydrologically basedmodel of land surface water and energy fluxes for general circulation models. J. Geophys. Res. 99 (D7), 14415–14428.

Mann, H.B., 1945. Nonparametric tests against trend. Econometrica 13 (3), 245–259.

Mao, X.S., Hu, C.S., Dou, M.J., Hou, Z.J., 2003. Dynamic observation and analysis moisture and temperature field coupling process in freezing soil. J. Glaciol. Geocryol. 25 (1), 55–59 (in Chinese).

Marchenko, S.S., Gorbunov, A.P., Romanovsky, V.E., 2007. Permafrost warming in the Tien Shan Mountains. Central Asia. Global Planetary Change 56 (3/4), 311–327.

Martin-Vide, J., 2004. Spatial distribution of a daily precipitation concentration index in peninsular Spain. Int. J. Climatol. 24, 959–971.

McClelland, J.W., Holmes, R.M., Peterson, B.J., Stieglitz, M., 2004. Increasing river discharge in the Eurasian Arctic: consideration of dams, permafrost thaw and fires as

potential agents of change. Journal of Geography Research 109, D18102. https://doi.org/10.1029/2004JD004583.
McGuire, A.D., 2002. Environmental variation, vegetation distribution, carbon dynamics and water/energy exchange at high latitudes. J. Veg. Sci. 13 (3), 301–314.
McNamara, J.P., Kane, D.L., Hinzman, L.D., 1998. An analysis of streamflow hydrology in the Kuparuk River basin, arctic Alaska: a nested watershed approach. J. Hydrol. 206, 39–57.
Nicolsky, D.J., Romanovsky, V.E., Alexeev, V.A., Lawrence, D.M., 2007. Improved modeling of permafrost dynamics in a GCM land-surface scheme. Geophys. Res. Lett. 34, L08501. https://doi.org/10.1029/2007GL029525.
Olascoaga, M.J., 1950. Some aspects of argentine rainfall. Tellus 2, 312–318.
Osterkamp, T., Romanovsky, V.E., 1997. Freezing of the active layer on the coastal plain of the Alaskan Arctic. Permafr. Periglac. Process. 8, 23–44.
Peterson, B.J., Holmes, R.M., McClelland, J.W., Vörösmarty, C.J., Lammers, R.B., Shiklomanov, A.I., Rahmstorf, S., 2002. Increasing river discharge to the Arctic Ocean. Science 298, 2171–2173.
Pomeroy, J.W., Gray, D.M., Brown, T., Hedstrom, N.R., Quinton, W.L., Granger, R.J., Carey, S.K., 2007. The cold regions hydrological process representation and model: a platform for basing model structure on physical evidence. In: Hydrological Processes. Vol. 21 (19). pp. 2650–2667.
Qian, Y.P., Lin, Y.P., Jin, S.Y., Jiang, X.H., 2004. Analysis of water resources changes in the source region of Yellow River. Water Resources and Hydropower Engineering 35 (5) 8–10. (in Chinese).
Riehl, H., 1949. Some aspects of Hawaiian rainfall. B. Am. Meteorol. Soc. 3, 176–187.
Romanovsky, V.E., Osterkamp, T.E., 1995. Interannual variations of the thermal regime of the active layer and near-surface permafrost in northern Alaska. Permafr. Periglac. Process. 6, 313–335.
Romanovsky, V.E., Osterkamp, T., 1997. Thawing of the active layer on the coastal plain of the Alaskan Arctic. Permafr. Periglac. Process. 8, 1–22.
Romanovsky, V.E., Osterkamp, T.E., 2001. Permafrost: changes and impacts. In: Paepe, R., Melnikov, V. (Eds.), Permafrost Response on Economic Development, Environmental Security and Natural Resources. Kluwer Academic Publishers, pp. 297–315.
Shao, Q.Q., Fan, J.W., 2012. The monitoring and evaluation on the ecosystem of Three-River Source Region. Science Press, Beijing (in Chinese).
Shao, J.A., Shao, Q.Q., Liu, Z.Y., 2009. Soil property and its formation of ecosystems in three river sources. Qinghai. Geographical Research 28 (3), 613–624 (in Chinese).
Shaw, G., Wheeler, D., 1994. Statistical Techniques in Geographical Analysis. Halsted Press, New York.
Shiklomanov, N., Nelson, F., Streletskiy, D., et al., 2008. The Circumpolar Active Layer Monitoring (CALM) program: Data collection, management, and dissemination strategies. In: Kane, D.L., Hinkel, K.M. (Eds.), Proc 9th Int Conf Permafrost. Vol. 2. pp. 1–6.
Shiklomanov, N.I., Streletskiy, D.A., Nelson, F.E., et al., 2010. Decadal variations of active-layer thickness in moisture-controlled land- scapes, Barrow, Alaska. J. Geophys. Res. 115, G00I04. https://doi.org/10.1029/2009JG001248.
Singh, P., Singh, V.P., 2001. Snow and Glacier Hydrology. Kluwer Academic publishers, Dordrecht, The Netherlands.
Tranter, M., Jones, H.G., 2001. The chemistry of snow: processes and nutrient cycling. In: Jones, H.G., Pomeroy, J.W., Walker, D.A., Hoham, R. (Eds.), The Ecology of Snow. Cambridge, UK, pp. 127–167 Cambridge University Press.
U.S. Arctic Research Commission Permafrost Task Force (ARCPTF), 2003. Climate change, permafrost, and impacts on civil infrastructure. In: Special Report 01–03. Arctic Research Commission, Arlington, VA, U.S..
Walker, D.A., Jia, G.J., Epstein, H.E., 2003. Vegetation-soil–thaw-depth relationships along a low-arctic bioclimate gradient, Alaska: synthesis of information from the ATLAS studies. Permafr. Periglac. Process. 14, 103–123.
Wang, T.M., Wu, G.X., Wan, R.J., 2008. Influence of the mechanical and thermal forcing of Tibetan plateau on the circulation of the Asian summer monsoon area. Plateau Meteorology 27, 1–9 (in Chinese).
Woli, K.P., Hayakawa, A., Kuramochi, K., Hatano, R., 2008. Assessment of river water quality during snowmelt and base flow periods in two catchment areas with different land use. Environ. Monit. Assess. 137 (1–3), 251–260.
Wu, Q.B., Zhang, T.J., 2010. Changes in active layer thickness over the Qinghai–Tibetan plateau from 1995 to 2007. J. Geophys. Res. 115, D09107. https://doi.org/10.1029/2009JD012974.
Xue, Y., Sellers, P.J., Kinter, J.L., 1991. A simplified biosphere model for global climate studies. J. Clim. 4 (3), 345–364.
Yang, K., Wu, H., Qin, J., Lin, C.G., Tang, W.J., Chen, Y.Y., 2014. Recent climate changes over the Tibetan plateau and their impacts on energy and water cycle: a review. Glob. Planet. Chang. 112, 79–91.
Yi, S., McGuire, A.D., Harden, J., Kasischke, E., Manies, K., Hinzman, L., Liljedahl, A., Randerson, J., Liu, H., Romanovsky, V., Marchenko, S., Kim, Y., 2009. Interactions between soil thermal and hydrological dynamics in the response of Alaska ecosystems to fire disturbance. J. Geophys. Res. 114, G02015. https://doi.org/10.1029/2008JG000841.
Yi, X.S., Li, G.s, Yin, Y.Y., Wang, B.L., 2012. Preliminary study for the influences of grassland degradation on soil water retention in the source region of the Yellow River. Journal of Natural Resources 27 (10), 1708–1719 (in Chinese).
Zhang, T.J., Barry, R.G., 2003. Changes in freeze–thaw and permafrost dynamics and their hydrological implication over the Russian Arctic Drainage Basin. The Proceedings of Freshwater Investigators Meeting, Boulder, February, In, pp. 18–19. http://arcticchamp.sr.unh.edu/abstracts/zhang.shtml.
Zhang, Y., Ohata, T., Kadata, T., 2003a. Land surface hydrological processes in the permafrost region of the eastern Tibetan plateau. J. Hydrol. 283, 41–56.
Zhang, Y., Kang, E., Ohata, T., 2003b. Observation and estimation of evaporation from the ground surface of the cryosphere in eastern Asia. Hydrol. Process. 17, 1135–1147.
Zhang, Y., Liu, C., Tang, Y., Yang, Y., 2007. Trends in pan evaporation and reference and actual evapotranspiration across the Tibetan plateau. J. Geophys. Res. 112 (D12110), 1–12.
Zhang, Q., Xu, C.Y., Marco, G., Chen, Y.P., Liu, C.L., 2009. Changing properties of precipitation concentration in the Pearl River basin. China. Stoch. Environ. Res. Risk. A. 23, 377–385.
Zhao, Y., Qian, Y.P., 2007. Relationships between the surface thermal anomalies in the Tibetan plateau and the rainfall in the Jianghuai area in summer. Chin. J. Atmos. Sci. 31, 145–154 (in Chinese).
Zhao, L., Wu, Q.B., Marchenko, S.S., et al., 2010. Thermal state of permafrost and active layer in Central Asia during the international polar year. Permafr. Periglac. Process. 21, 198–207.
Zhou, J., Kinzelbach, W., Cheng, G.D., Zhang, W., He, X.B., Ye, B., 2013. Monitoring and modeling the influence of snow pack and organic soil on a permafrost active layer, Qinghai–Tibetan plateau of China. Cold Reg. Sci. Technol. 90–91, 38–52.
Zhou, J., Pomeroy, J.W., Zhang, W., Cheng, G.D., Wang, G.X., Chen, C., 2014. Simulating cold regions hydrological processes using a modular model in the west of China. J. Hydrol. 509, 13–24.
Zhao, L., Wu, T.H., Xie, C.W., Li, R., Wu, X.D., Yao, J.M, Yue, G.Y., Xiao, Y., 2017. Support Geoscience Research, Environmental Management, and Engineering Construction with Investigation and Monitoring on Permafrost in the Qinghai-Tibet Plateau, China. Bull. Chin. Acad. Sci. 32 (10), 1159–1168.
Zhuang, Q., Melillo, J., Kicklighter, D., Prinn, R.G., McGuire, A.D., Steudler, P.A., Felzer, B.S., Hu, S., 2004. Methane fluxes between terrestrial ecosystems and the atmosphere at northern high latitudes during the past century: a retrospective analysis with a process-based biogeochemistry model. Glob. Biogeochem. Cycles 18, GB3010. https://doi.org/10.1029/2004GB002239.